Sizing of an Entry, Descent, and Landing System for Human Mars Exploration

John A. Christian[*], Grant Wells[†], Jarret Lafleur[‡], Kavya Manyapu[‡], Amanda Verges[‡], Charity Lewis[‡],
and Robert D. Braun[§]
Georgia Institute of Technology, Atlanta, GA, 30332-0150

The human exploration of Mars presents many challenges, not least of which is the task of entry, descent, and landing (EDL). Because human-class missions are expected to have landed masses on the order of 40 to 80 metric tons, significant challenges arise that have not been seen to date in robotic missions. This study provides insight into the challenges encountered as well as potential solutions through parametric trade studies on vehicle size and mass. Aerocapture and entry-from-orbit analyses of 10 and 15 m diameter aeroshells with a lift-to-drag ratio of 0.3 or 0.5 were investigated. Results indicate that in the limit, a crew capsule used only for descent could have an initial mass as low as 20 t. For larger landed payloads, such as a 20 t surface power system, a vehicle with an initial mass on the order of 80 t may be required. In addition, no feasible EDL systems were obtained with the capability to deliver more than approximately 25 t of landed payload to the Mars surface for initial masses less than 100 t. This suggests that an aeroshell diameter of 15 m may not be sufficient for human Mars exploration.

Nomenclature

a_D	=	instantaneous acceleration due to drag
a_T	=	instantaneous acceleration due to thrust
g	=	local acceleration due to gravity
g_0	=	acceleration due to gravity on Earth's surface (9.81 m/s)
h	=	altitude
m_{engine}	=	engine mass
D	=	aerodynamic drag
I_{sp}	=	specific impulse
L	=	aerodynamic lift
T	=	thrust
V	=	velocity
ψ	=	nadir angle
ΔV	=	change in velocity

I. Introduction

NASA's Vision for Space Exploration[1] clearly states the agency's long-term desire to send humans to Mars. In the years since Mariner 4 became the first successful mission to reach Mars in 1965, much progress has been made by a robust robotic Mars exploration program in both the United States and abroad. To date, the United States has successfully landed 5 robotic spacecraft on the surface of the red planet. All of these vehicles, however, have been quite small, with landed masses no greater than 600 kg. It is estimated that human missions require landed

---

[*] Graduate Teaching Assistant, Guggenheim School of Aerospace Engineering, AIAA Student Member.

[†] Graduate Research Assistant, Guggenheim School of Aerospace Engineering, AIAA Student Member.

[‡] Undergraduate Student, Guggenheim School of Aerospace Engineering, AIAA Student Member.

[§] David and Andrew Lewis Associate Professor of Space Technology, Guggenheim School of Aerospace Engineering, AIAA Associate Fellow.

masses on the order of 40 to 80 metric tons.[2] This will involve landing approximately two orders of magnitude more mass on the Martian surface in a single landing than has been achieved to date. Such a task is not to be taken lightly. Indeed, among the most difficult tasks in any mission to the Martian surface is Entry, Descent, and Landing (EDL).

The EDL systems proposed in this paper are designed to be capable of landing human-class payloads on Mars. Restrictions placed on the vehicle (such as deceleration limits) make these systems suitable for crewed descent, although they could also be configured to deliver cargo. This study includes the examination of a number of possible descent scenarios, sequences, and trajectories in conjunction with the required hardware. Using an Apollo-like capsule (blunt body with sidewall angle of 32º) and assuming a conservative atmosphere as a baseline, this study performs two sweeps of vehicle mass and size for each scenario: one at an angle of attack of -21.7º (hypersonic lift-to-drag ratio of 0.3) and one at an angle of attack of -40.8º (hypersonic lift-to-drag ratio of 0.5). This information is employed to size the EDL system with the objective of achieving the greatest landed mass for a given entry mass. Here, analysis focuses on sizing of the ablative thermal protection system, aeroshell, parachute system, propulsion system (including tanks and engine), reaction control system and other subsystems. The study is concluded by placing these findings in context of proposed human Mars architectures and the Vision for Space Exploration. While most estimates place the first human mission to Mars more than 25 years in the future, there is a serious need to begin work today. Knowledge gained now may be leveraged to guide robotic precursors, maximize the return from lunar testing, and improve current human Mars mission concepts.

II.   Overview of Martian Environment

A. Atmosphere Model

The atmospheric density on Mars varies significantly with season, dust content, position (latitude), and time of day. These parameters were randomly varied for 1000 cases using Mars-GRAM 2005 in order to create atmosphere profiles. Mars-GRAM is a widely used Mars atmospheric model which uses the MOLA (Mars Orbiter Laser Altimeter) reference altitude, measured from data collected on the Mars Global Surveyor spacecraft.

Cumulative distribution functions of density were constructed for each altitude from -8 km to 152 km MOLA. The density at the 30% point for the 0 km cumulative distribution function was chosen. Using this 0 km 30% value, the atmosphere with the lowest 4 km density was baslined. This atmosphere satisfies hydrostatic equilibrium, resulting in a realistic and conservative atmosphere. The resulting density profile gives a MOLA 0 km density of 0.012439 kg/m³. Approximately 70% of the atmospheric density profiles simulated had a higher 0 km density. This baseline density profile is shown in Figure 1.
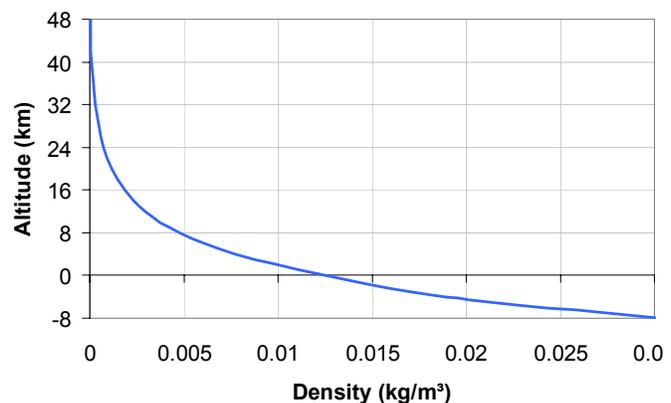

Figure 1. General Density Profile.

III.   Baseline Mission Profile

The baseline mission profile investigated in this study begins by inserting the crewed spacecraft into orbit around Mars using aerocapture. After aerocapture, propulsive maneuvers insert the vehicle into an acceptable parking orbit and then deorbit the vehicle when it is ready to descend to the Martian surface. After a lifting entry, the capsule continues to decelerate (both with and without parachutes) until the initiation of a propulsive descent phase. This powered flight phase continues until the vehicle safely touches down on the surface of Mars. The EDL systems explored within this study were designed to accommodate landing sites with elevations at or below 0 km MOLA.

A. Aerocapture

Aerocapture slows a spacecraft from hyperbolic to orbital speed in a single pass through the atmosphere of a planet. An aerocapture schematic is provided in Figure 2. The spacecraft was assumed to enter the atmosphere with a velocity of 6 km/s. This is a lower velocity in a wide range of interplanetary trajectory options.[3] The target post-aerocapture orbit for this investigation was an elliptical orbit with a semi-major axis of approximately 5,212 km and an eccentricity of 0.34. The aerocapture trajectory was simulated using the Program to Optimize Simulated

Trajectories (POST)[4] and flown with lift down for both an L/D of 0.3 and an L/D of 0.5. A lift-down trajectory was chosen for aerocapture because these trajectories give the lowest peak deceleration and it was assumed that the crew would be deconditioned and unable to tolerate high accelerations after the interplanetary transit.

B. Orbital Maneuvering

After the aerocapture maneuver, a ΔV is performed at apoapsis to raise periapsis and establish an elliptical parking orbit (Figure 2). The crew will remain in this orbit until ready to descend to the surface. Additionally, orbiting assets (such as the vehicle required to carry the crew back to Earth) could be placed in this type of orbit. From this orbit, another propulsive ΔV is used to deorbit the craft (Figure 2) such that it meets the 4 km/s entry velocity and approximate -14.5° flight path angle dictated by the selected undershoot entry condition.

Together these maneuvers have the potential of being quite expensive. The post-aerocapture semi-major axis and the relative orientation of the deorbit and parking orbits was varied such that the sum of parking orbit insertion and deorbit burns is minimized. The post-aerocapture orbit is constrained to a 3,440 km apoapsis radius due to aerocapture considerations while the parking orbit is constrained to a 3,780 km periapsis radius in order to maintain a safe 400 km periapsis altitude[**][††]. This optimization results in a 63.8 m/s ΔV to raise periapsis and enter a parking orbit with an eccentricity of 0.3 and a 137.6 m/s ΔV to initiate the deorbit maneuver. A 25% ΔV margin is applied, resulting in an optimized ΔV of 251.8 m/s.
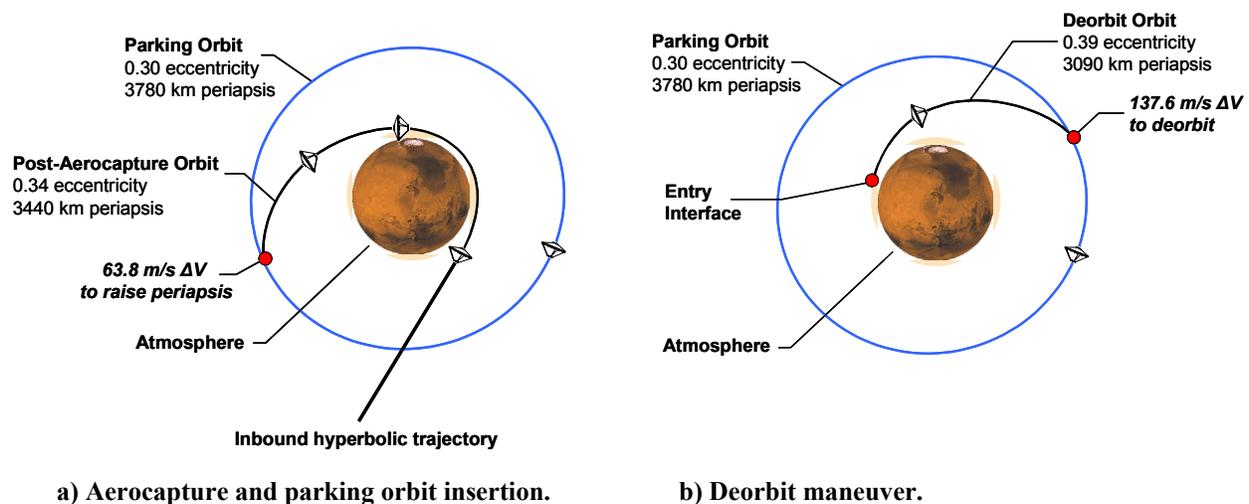

a) Aerocapture and parking orbit insertion.   b) Deorbit maneuver.

Figure 2. Aerocapture and orbital maneuvers.

C. Entry

For the purposes of this study, an entry-from-orbit velocity of 4 km/s is targeted in order to determine the entry corridor based on: (a) the lift-down trajectory with the most shallow flight path angle that allows for entry without skipping out (the overshoot trajectory) and (b) the lift-up trajectory with the steepest flight path angle having a peak deceleration of 5 g (the undershoot trajectory). The 5 Earth-g limit is considered the maximum deceleration that a deconditioned human crew can tolerate for short durations.[5] The flight path angle range between the lift-down and lift-up trajectory angles provides a navigable entry corridor.

Entry and non-propulsive descent trajectories are computed using the three-degree-of-freedom version of POST. This tool allows for trajectory optimization based on specified lift-up or lift-down conditions achieved through various entry angles. POST also allows for the modeling of deployables such as parachutes.

[**] For reference, Mars Odyssey planned for a circular final orbit with a 400 km altitude,[6] and Mars Global Surveyor planned for a final orbit with a 378 km mean altitude.[7]
[††] An additional optimization routine is used to vary post-aerocapture and parking orbit periapsis in order to minimize total ΔV. These periapsis constraints were chosen since results indicate that post-aerocapture periapsis should be as high as practicable and parking orbit periapsis should be as low as practicable.

D. Descent

Two types of descent sequences were investigated: one that uses parachutes and one that does not . When using a parachute, the vehicle deploys a 30 m diameter disk-gap-band (DGB) parachute at Mach 3. A DGB parachute was chosen due to its proven performance at supersonic velocities in low density environments. The parachute was not allowed to grow beyond 30 m due to performance and fabrication concerns.[2] Additionally, the parachute was not permitted to begin deployment before Mach 3 due to aeroheating and area oscillation concerns in regimes approaching March 3 (deployment and inflation tests have been successfully performed up to about Mach 2.7[8]). Descent scenarios that do not employ a parachute system make up the difference in deceleration propulsively during the powered descent phase.

Previous studies have suggested[6,7] that, even with optimistic parachute assumptions, a substantial propulsive descent capability is required for any human-class Mars landing mission. In order to estimate corresponding propellant and propulsion system mass requirements, propulsive descent analysis is performed by numerically integrating the nonlinear differential equations of motion of the gravity-turn control law. This control law was originally developed for the 1966-1968 lunar Surveyor landings and specifies that a spacecraft's thrust vector is maintained in the orientation opposite its velocity vector. Typically, the termination of a gravity turn is when the nadir angle, relative velocity, and height above ground level are all zero or the requisite values.

For the purposes of this study, two-dimensional gravity turn trajectories are assumed to occur over a flat Mars. The free body diagram and associated equations of motion are shown in Figure 3 and Eqs. (1).
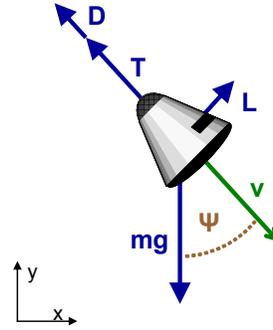

Figure 3. Gravity Turn Free Body Diagram.

Two force equations can be developed for the x and y directions, and these can be manipulated to yield Eqs. (1).

$$\dot{\psi} = \frac{a_L - g\sin\psi}{v}$$

$$\dot{v} = g\cos\psi - a_T - a_D \tag{1}$$

A final required relationship is a description of vehicle mass change over time. This is given by the definition of specific impulse, which can be rearranged to yield Eq. (2).

$$\dot{m} = -\frac{T}{g_0 I_{sp}} \tag{2}$$

The equations of motion are integrated over small timesteps to yield trajectory data and to generate thrust, ΔV, and propellant mass fraction requirements. Two significant assumptions of the implementation of this integration are
1) Lift is zero, as lift capabilities are assumed to be kept in reserve during propulsive descent.
2) Thrust is constant throughout the gravity turn, with no engine gimbaling. A study to optimize ΔV via throttling and gimbaling was performed on a sample case but showed only small differences in overall requirements. Further, ΔV optimization results are not shown since unmodeled considerations (e.g., range safety, winds, and density uncertainty) contribute substantially to the propellant requirements.

From a propellant mass perspective, it is desirable to begin the gravity turn burn as late as possible, which allows maximum aerodynamic deceleration and minimizes gravity loss. However, if the burn begins too late, thrust requirements become unreasonably large since lower Mach numbers also occur at lower altitudes, meaning the vehicle must zero its velocity in less and less time. Previous studies indicate that a thrust level of around 1.0 MN encompasses most reasonable cases of interest.

A simulation was developed that seeks to minimize the vehicle mass (minimizing the sum of the propellant mass and propulsion system mass) by altering the time at which the gravity turn is initiated. The primary constraint during

this optimization is a 5 Earth-g deceleration limit. Despite this constraint, none of the feasible cases investigated exhibited peak accelerations above 3.8 m/s^2.

To find the gravity turn initialization time that yields the minimum mass, the search algorithm used the POST trajectory discussed in the Section III.C. Starting at the ground and moving backwards in time, the search algorithm looks for the minimum propellant/propulsion system combined mass that satisfies the deceleration constraint. It should be noted that most of the optimized cases required a total vehicle thrust less than 1.0 MN, while a few cases on the extremes of the parametric search required total thrust levels that were slightly higher.

E. Landing

It is desired that a hover and cross-range capability be built in to the powered descent profile which allows for final landing maneuvering and hazard avoidance. The hover and cross-range maneuver shown in Figure 4 assumes a cross-range requirement of 500 m at a 50 m altitude and provides a conservative estimate on ΔV and propellant requirements. This maneuver consists of three parts: a cross-range acceleration, a cross-range deceleration, and a vertical descent. Equations of motion were developed and are evaluated in MATLAB after the termination of a gravity turn trajectory at 50 m MOLA altitude and zero velocity; typically, ΔV required for this cross-range maneuver is approximately 265 m/s.
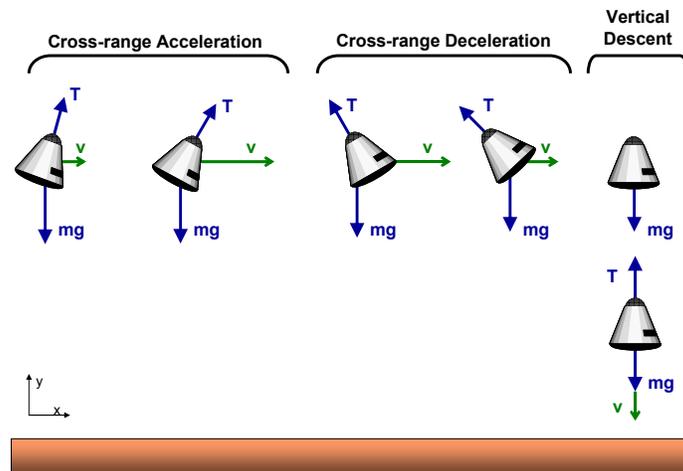

Figure 4: Hover and Cross-Range Maneuver.

IV. Vehicle Configuration

The Apollo-like blunt body shape presents a number of significant configuration challenges when used for human-class Mars missions. Major configuration issues were addressed in the areas of heatshield design, cargo unloading, and engine placement.

Most of the EDL challenges center around the heatshield design. The first hurdle is to determine if one or two heatshields will be required for the aerocapture and entry maneuvers. Due to the decision to use carbon-carbon over fiber-form as the TPS material (see section V.A for more details), a single heatshield was shown to provide better performance. However, it is estimated that fabrication limitations will prevent any one carbon-carbon panel from exceeding approximately 5 m in its largest dimension. The carbon-carbon sections, therefore, must be paneled to cover the 10 m and 15 m diameter vehicles, resulting in numerous seams along the windward side of the vehicle. While not desirable, these seams are not considered to be a showstopper. A graphical representation of how the carbon-carbon tiling may be configured is shown below in Figure 5.
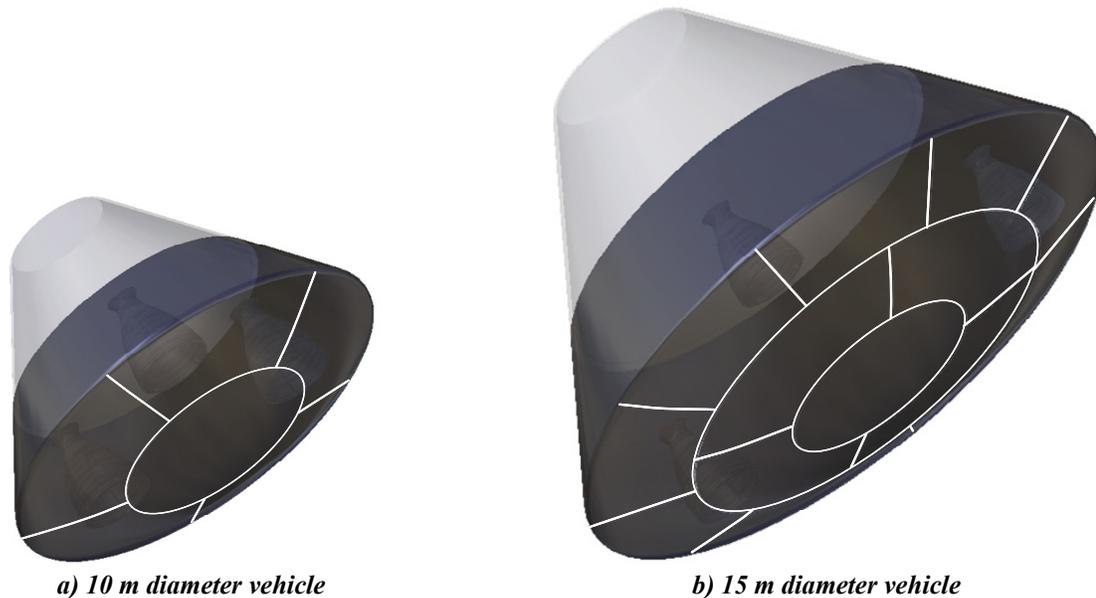
a) 10 m diameter vehicle   *b) 15 m diameter vehicle*

Figure 5: Carbon-carbon tile configuration for 10 m and 15 m diameter vehicle.

After entry, the heatshield must be moved to expose the descent engines. At least two options are available to expose the descent engines: (1) the vehicle may drop the heatshield prior to engine ignition or (2) doors may be opened in the heatshield to expose the engines. Significant challenges were encountered in both of these options. For the first option, the ballistic coefficient of the vehicle is greater than that of the heatshield (even with a 30 m DGB parachute deployed). Until the ballistic coefficient of the heatshield becomes greater than that of the remainder of the vehicle it will remain pressed against the bottom of the vehicle. Under these conditions, if the heatshield does become separated from the vehicle there is a significant risk of recontact between the heatshield and the vehicle/parachute. The second option (doors in the heatshield to expose engines) requires additional seams and/or penetrations in the heatshield, adding complexity and potential failure modes. Other options that were assessed, but dismissed as too complex or risky, include the following:

1. Engines that deploy off the side or top of the vehicle. This was seen as too complicated with too many failure points to be acceptable for a human mission.
2. Engines facing towards the leeward side of the vehicle (engine bells at or near the apex of the cone). This would require the crew to experience a 180º rotation during the EDL sequence, creating unacceptable crew acceleration conditions. Note that the crew would end the EDL sequence facing the opposite direction of the way they started (i.e. the acceleration during entry may be eyeballs-in, while acceleration during powered descent would be eyeballs-out).

Cargo unloading on the Martian surface also imposes configuration challenges. The first problem is unloading the cargo from a high platform above the surface. Due to the landing gear and the size of the engines and propellant tanks, it is unlikely that the cargo will be very close to the Martian surface. One of the major advantages of the 15 m diameter vehicle is the significant increase in space that would allow the cargo to be placed lower to the ground. A second problem relates to the vehicle backshell: is the backshell dropped prior to landing? Here, the driving case is considered to be a crewed vehicle or one with a pressurized payload. In this scenario, as has been shown in previous studies,[8] significant mass, volume, and complexity penalties may be incurred by separating the backshell from the pressure vessel and primary structure. The baseline configuration, therefore, employs a backshell that is integral to the vehicle's primary structure and is not discarded.

Descent engine configuration presents a number of interesting challenges for a vehicle of this shape. A configuration trade was performed that investigates the use of one large engine or multiples of smaller engines for the 10 m and 15 m diameter vehicles (see Figure 6 and Figure 7, respectively).

Figure 6: Engine configuration options for 10 m diameter vehicle.

Figure 7: Engine configuration options for 15 m diameter vehicle.

A review of Figure 6 and Figure 7 shows that the 4-engine options creates for the largest amount of useful area for the payload and propellant tanks while allowing ample space for access to the vehicle's outer wall. This option could also allow for some engine-out capability if each engine has sufficient gimbaling authority. Note that engine clusters consisting of more than four engines were not considered due to concerns of increasing system complexity.

V.   EDL Subsystem Sizing Methodology

A. Heatshield Sizing

Heatshield mass estimation consisted of two distinct segments. The first involved calculating the mass of the TPS material required to protect the vehicle during Mars aerocapture and entry, while the second provided a mass estimate of the underlying structure. The TPS mass was estimated by calculating the required TPS thickness and insulation thickness at the stagnation point of the heatshield (computed using 1-D finite difference heat transfer calculations). A previous study by the authors[7] selected the ablative material PICA (phenolic impregnated carbon ablators) for the TPS material. Due to concerns with manufacturing large, relatively thick panels of PICA, carbon-carbon over fiber form was chosen for this study. Additionally, it is worth noting that carbon-carbon experiences no recession over the temperatures experienced during Mars aerocapture or entry for any of the cases investigated.

In determining the TPS mass, the carbon-carbon was assumed to be 1 mm thick (density of 1890 kg/m^3) and the thickness of the fiber-form insulation (density of 180 kg/m^3) was chosen such that the temperature at the bondline remained below 250º C at all times. This maximum temperature was selected due to limitations of the bondline

adhesive. The underlying heatshield structure was estimated as 10% or 15% of the total entry mass for the 10 m or 15 m diameter vehicles, respectively.

B. Parachute System Sizing

One of the problems investigated in this study is the feasibility of using parachutes in the descent sequence for human-scale Mars missions. With this in mind, the model used to estimate the parachute mass becomes very important. As with previous Mars missions, a DGB parachute was selected for its proven performance at Mars. Material strength and stability concerns led to a limit on the parachute diameter of 30 m. All of the cases investigated in this study pushed up against this limit and required a 30 m diameter parachute.

A parachute sizing tool was developed to estimate parachute mass. Canopy, suspension line, and riser masses are estimated based on material selection, parachute size, and the vehicle mass. The mortar mass was estimated based on historical mortar data. A simple regression analysis shows that the mortar mass may be estimated by $M_m=2.2M_p^{0.5}$, where M_m is the mortar mass and M_p is the parachute mass.[11] The mass of suspension lines, risers, and tapes were sized to withstand the maximum expected load with a factor of safety of 1.5. Due to the high vehicle mass relative to parachute size, an infinite mass inflation was assumed with peak loads occurring at full inflation. These expected loads were estimated using the C_k-method with C_k values derived from historical DGB data.[13]

C. Backshell and Structure

Given the nature of human Mars missions, it was not clear that a significant benefit could be gained by dropping the backshell as has been done on recent robotic missions. Experience with crewed capsule-type vehicles (Apollo, Soyuz, etc.) as well as human Mars architecture studies (Mars DRM 3.0[10]) suggest that mass, volume, and complexity benefits may be gained through the use of a backshell that is integral with the primary structure. Such a design was employed in this study. The backshell and primary vehicle structure was assumed to constitute 25% of the vehicle dry mass.

D. Propulsion System Sizing

The propulsion system used during the powered flight portion of the EDL sequence will employ a liquid bipropellant engine using methane (CH_4, density of 422.6 kg/m^3) and liquid oxygen (LOX, density of 1140.1 kg/m^3). A LOX/CH4 propulsion system was chosen to remain consistent with the majority of previous human Mars exploration studies.[10,12] This propellant combination is advantageous for Mars missions because of the relative ease by which carbon dioxide in the Martian atmosphere may be converted to methane through the Sabatier reaction ($CO_2 + 4 H_2 \rightarrow CH_4 + 2 H_2O$). The methane produced at Mars through this process may be used as propellant for the crew's ascent vehicle or other devices surface devices (such as LOX/CH4 fuel cells). For maximum commonality with the ascent vehicle, it is desirable to use the same propellant (or even engines) on both the descent vehicle and ascent vehicle. Finally, it was assumed that the LOX/CH4 engine used on this vehicle would have a specific impulse on the order if 350 seconds at a mixture ration of 3.5.

The propulsion system sizing algorithm assumes a rubberized engine with a mass dictated by the relationship shown in Eq. (3). This expression is the result of a simple regression analysis performed on thrust vs. mass data for a number of conceptual LOX/CH4 engines.

$$m_{engine} = 0.00144*T + 49.6 \qquad (3)$$

Note that this equates to an average engine thrust-to-weight ratio (on Earth) of about 67 for the vehicles investigated in this study. Additionally, propellant tanks were assumed to be made of titanium and have an operating pressure of approximately 1.38 MPa (burst pressure of ~2.76 MPa).

E. Orbital Thruster and Reaction Control System Sizing

The orbital maneuvering system (OMS) and reaction control system (RCS) provide orbital maintenance and vehicle orientation capability. The 12-thruster configuration used in both vehicles is based on the configuration used by Apollo command module. A hypergolic RCS system, using monomethyl hydrazine (MMH, density of 878 kg/m3)[14] and nitrogen tetroxide (N_2O_4, density of 1440 kg/m3),[14] was chosen for historical reasons – most RCS systems designed to date have relied on hypergolic propellants for simplicity and reliability. Each individual thruster was assumed to have a mass of 3.8 kg, operate at a mixture ratio of 2.16, and have a specific impulse of approximately 289 seconds. The propellant tanks were sized in a fashion similar to that of the main propulsion system.

F. Command, Control, and Communications (C^3)

Communication with the vehicle will be required during transit to Mars, during the time between aerocapture and entry, and after entry. It was estimated that the required data rates to fulfill mission needs will be on the order of 10s of kbps, although the required data rate may be highly variable. For the crewed version of this vehicle, a higher data rate may be required (video transmissions may require data rates up to 10s of Mbps[15]), although the high bandwidth communication required for this mission would be book kept separately under the human-specific payload. The baseline communications will consist of a 100 kbps X-band link (8 GHz) that will utilize a network that possesses capability similar to that of the Deep Space Network. From a mass sizing standpoint, it was assumed that the vehicle will carry two amplifiers, two transponders, one primary high-gain antenna, and two smaller low-gain antennas.

G. Power

It was assumed that power is provided by an outside source (service module or cruise stage type device) during the transit from Earth to Mars. Once in the Mars vicinity, the vehicle must separate from the service module to prepare for aerocapture. From this point forward, the vehicle must provide power to run critical systems and support the payload. It was assumed that LOX/LH2 fuel cells would provide power for up to 72 hours after separation from the service module to allow time for aerocapture, on-orbit checkout, and landing site phasing (LOX/CH4 fuel cells are also worth investigating if methane remains a top fuel choice for the descent or ascent vehicle). The LOX/LH2 fuel cells were assumed to consume 0.34 kg of O_2 and 0.05 kg of H_2 while producing 0.36 kg of H2O for every kW-hr of energy produced. Additionally, assuming shuttle-class fuel cells, each fuel cell unit would to have a mass of 91 kg and be capable of producing approximately 4.7 kW (peak of 12 kW).[15]

Prior to entry, the fuel cells will be shut-down and power will be drawn from a bank of lithium-ion batteries for a period of approximately 12 hours. This should provide sufficient time for entry, descent, and landing followed by initialization of (or connection to) the surface power source. The lithium-ion batteries were assumed to have an energy density of 0.15 kW-hr/kg.

To support a human crew or a large payload, it was assumed that the vehicle must be capable of supplying approximately 9 kW of electrical power.

H. Landing Hardware

Some form of landing hardware will be required for the vehicle to make a soft touchdown on the Martian surface. Because this vehicle will carry the crew and other potentially sensitive payloads, landing gear was chosen over other options such as airbags or crushable material. Furthermore, it was assumed that the landing gear mass scales linearly with the vehicle's landed mass. For the purposes of this study, the landing gear mass is approximated as 3% of the vehicle landed mass.[16]

I. Mass Margin

Given the parametric nature of the designs presented in this study, all subsystem mass estimates are very preliminary. Given the high degree of uncertainty in how subsystem masses may change as potential designs mature, a mass contingency of 30% was applied to the vehicle dry mass.

VI.   Trade Study Results

The surface payload capability for each scenario investigated is shown in Figure 8 and Figure 9. When reviewing these results, first note that payload mass increases nearly linearly with an increase in initial mass for the cases where no parachute is used (black line, propulsive only descent). The cases that make use of a parachute (red line) show slightly better performance over the range of masses investigated, but become less efficient as the vehicle mass increases. In all the cases investigated, the maximum benefit gained by using a parachute is 1.9 t. Also note that some curves end before reaching an initial mass of 100 t. The data points not plotted represent cases where the gravity turn was forced to begin unrealistically early to meet the established thrust and acceleration limits. In these cases, the burn time is long and the propellant lost due to gravity effects is substantial. The large increase in required propellant mass results in the mass of the other subsystems exceeding the available dry mass for the specified initial mass, an infeasible result.
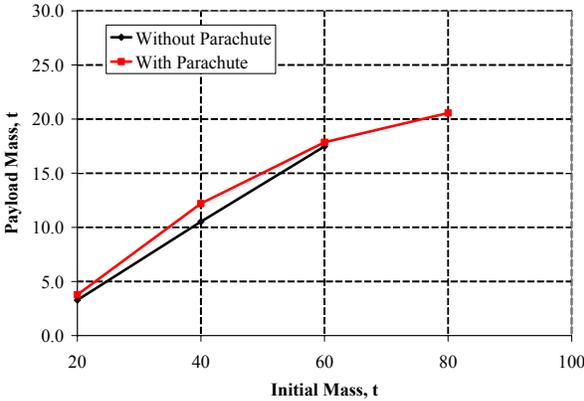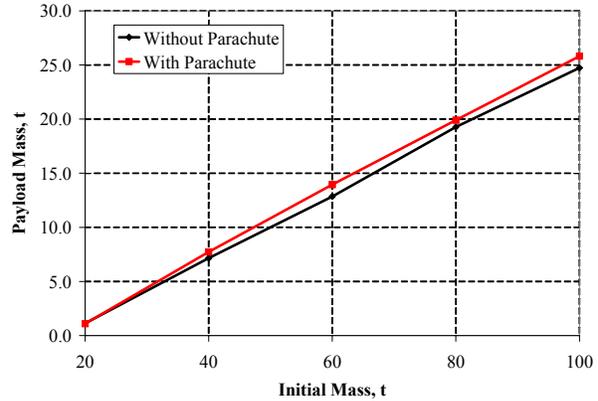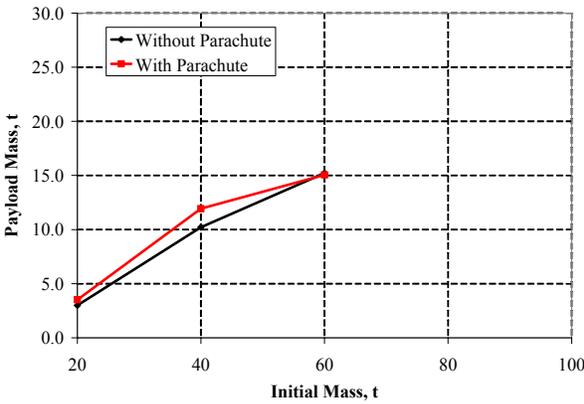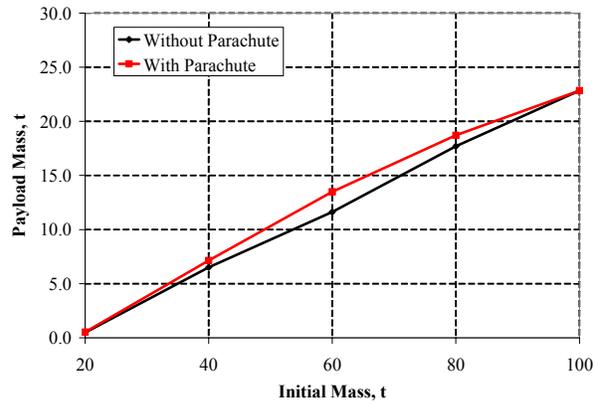
a) 10 m diameter vehicle   *b) 15 m diameter vehicle*

Figure 8: Payload delivered to the Martian surface for L/D=0.3.

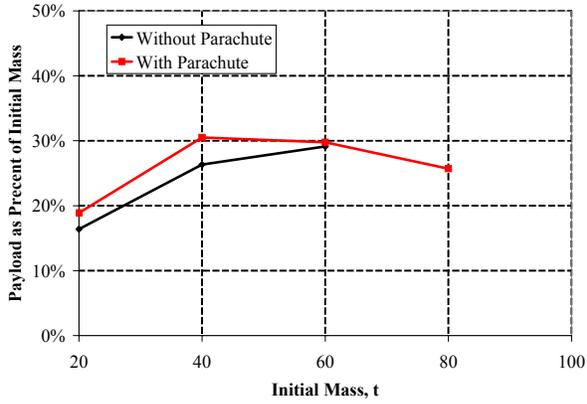*a) 10 m diameter vehicle*   *b) 15 m diameter vehicle*

Figure 9: Payload delivered to the Martian surface for L/D=0.5.

Comparing the results of the L/D=0.3 and L/D=0.5 cases, it is observed that the cases with the lower L/D can land slightly larger payloads on the Martian surface. The L/D=0.5 cases, when flown on the pure lift-up entry profiles used in this study, lead to shallower and faster trajectories. This results in the optimal point for the gravity-turn initiation to occur at a higher velocity, leading to a lower landed payload mass.

The environmental control and life support system (ECLSS) required to support a crew of six for three days has a mass of approximately 2 t. Carrying the crewmembers themselves will require an additional metric ton. Therefore, using the graphs above, it is estimated that in the limit, a crew capsule used only for descent could have an initial mass as low as 20 t. Other payloads, such as the ~20 t surface power system proposed in the ESAS study,[17] would require a vehicle with an initial mass on the order of 80 t. Note that a larger diameter vehicle may also be required to land payloads of this mass. In addition, no feasible cases were obtained with the capability to deliver more than approximately 25 t of payload to the Mars surface for initial masses less than 100 t.

It is also useful to view this data in terms of percentage of the vehicle's initial mass. This data is shown below in Figure 10 and Figure 11. Note that vehicles with initial masses between 40 t and 80 t deliver landed payloads on the order of 15% to 30% of the initial mass.

To gain a feel for individual subsystem contributions to the overall vehicle mass, two example pie charts are shown in Figure 12 for the 15 m diameter, 60 t vehicle flown at an L/D of 0.3.
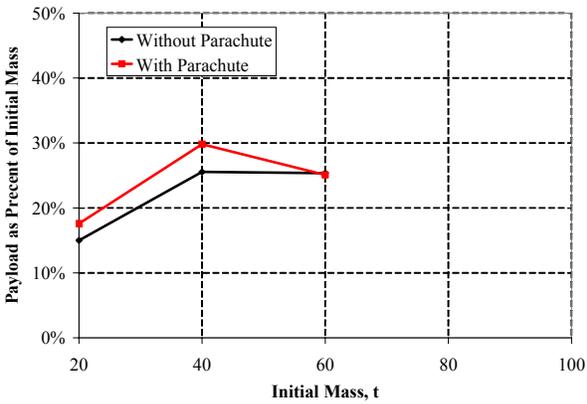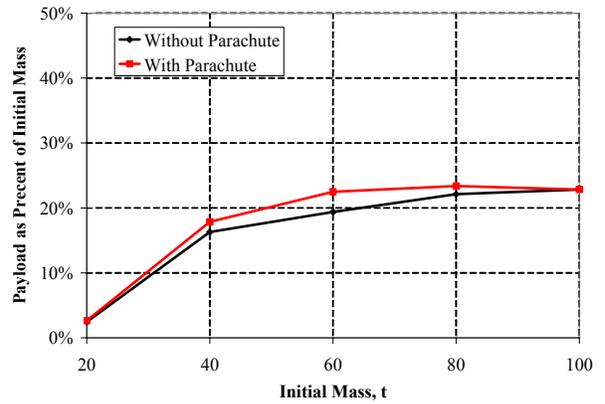
a) 10 m diameter vehicle
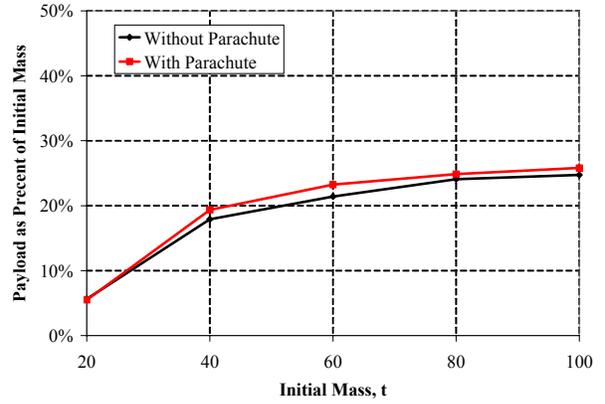
b) 15 m diameter vehicle

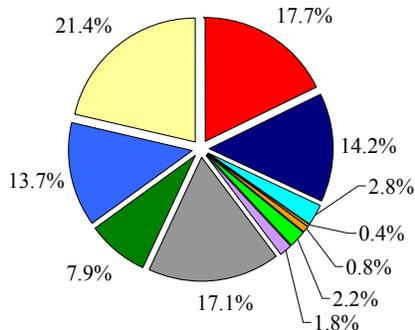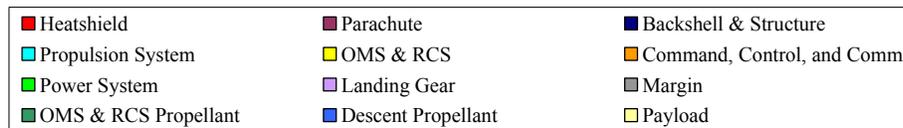**Figure 10: Payload delivered to the Martian surface as percentage of initial mass for L/D=0.3.**
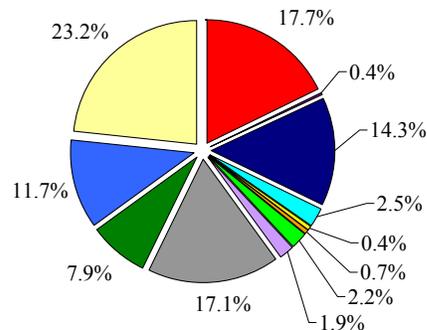

a) 10 m diameter vehicle

b) 15 m diameter vehicle

Figure 11: Payload delivered to the Martian surface as percentage of initial mass for L/D=0.5.

a) Vehicle without parachute

b) Vehicle with parachute

Figure 12: Mass breakdown for 15 m diameter, 60 t vehicle for L/D=0.3.

VII. System-Level Implications

Given the four-engine configurations shown in Figure 6 and Figure 7, pressurized volumes will not be able to exceed approximately 60 m^3 and 287 m^3 in the 10 m and 15 m diameter vehicles, respectively. A significant portion of this pressurized volume will be taken up by cargo, crew accommodations, and other subsystems, resulting in a habitable volume that is noticeably lower. According to NASA-STD-3000,[5] a six-person crew would require a habitable volume of no less than ~60 m^3 (with optimal performance at habitable volumes greater than ~120 m^3) for durations on the order of the transit time from Earth to Mars. Based on these criteria, the crew would need a separate habitat for the transit to and from Mars if the 10 m diameter vehicle was chosen. Additionally, it should be noted that if the capsule were to be used as crew living quarters on the Martian surface, there is very limited floor space. Given the ceiling height required for humans to comfortably move about on the surface, even the 15 m diameter capsule only has a usable floor area of ~23 m^2. This underscores the need for a dedicated habitat for a human Mars mission.

Unfortunately, a rigid habitat of sufficient size cannot fit in the capsule shape. In order to land a habitat on the Martian surface, one of two approaches would be necessary: (1) use of an inflatable habitat or (2) flight of a separate entry system for the habitat and other large payloads.

Finally, the capsule diameter will strongly influence the launch vehicle. It is conceivable that a 10 m diameter launch vehicle may exist in the future; however, a 15 m diameter vehicle is much larger than anything currently available or in future plans. One option for large diameter capsules is on-orbit assembly, although such an endeavor may be prohibitive from a cost and complexity perspective.

VIII. Conclusions

This study explored, from a configuration and mass sizing perspective, how a traditional capsule shape may be used for the human exploration of Mars. The results suggest that vehicles with entry masses in the 40-80 t range would be capable of deploying cargo with a mass on the order of 5-20 t. This is equivalent to landed payload masses that account for only 15% to 30% of the initial mass. Note that the payload mass fractions presented here are much lower than has been assumed in many human Mars mission conceptual studies. Indeed, none of the cases investigated in this study were able to land a payloads with a mass exceeding about 25 t. This may become a significant concern if human mission surface components (habitat, power system, ISRU plant, rovers, etc.) cannot be separated into segments with sufficiently small masses. Future work should look into incorporating a detailed EDL design into existing Mars design reference missions to assess the system level impacts.

An additional challenge was shown to be habitable volume (during transit) and usable floor space (once landed on Mars). Due its sloped sidewalls, payload volume restrictions are seen to be one of the major drawbacks of the capsule shape. Despite its drawbacks, the capsule shape is a promising configuration for delivering the crew to the Martian surface. In future work, vehicles with other shapes (biconic, ellipsled, ballute, etc.) should be investigated as they may provide more packaging flexibility for large payloads. Care must be taken with slender body shapes so as to not sacrifice aerodynamic drag area and hence deceleration performance.

Acknowledgments

References

[1]   "Vision for Space Exploration," National Aeronautics and Space Administration, February 2004.

[2]   Braun, R.D., Manning, R.M., "Mars Exploration Entry, Descent and Landing Challenges," IEEE Aerospace Conference, Big Sky, MT, May 2006

[3]   Hofstetter, W.K., Wooster, P.D., Nadir, W.D., Crawley, E.F., "Affordable Human Moon and Mars Exploration through Hardware Commonality," AIAA-2005-6757, *Space 2005*, Long Beach, California, 30 Aug - 1 Sep 2005.

[4]   POST, Program to Optimize Simulated Trajectories, Ver. 5.2, NASA Langley Research Center, Hampton, Virginia, Martin Marietta Corporation, Denver, Colorado, 1997.

[5]   Man-Systems Integration Standards, Revision B, NASA-STD-3000, July 1995.

[6]   Lafleur, J., and Verges, A. "Parachutes and Propulsive Descent for Human Mars Exploration." AIAA Student Conference Paper. Starkville, 3-4 April 2006.

[7]   Wells, G., Lafleur, J., Verges, A., et al. "Entry, Descent and Landing Challenges of Human Mars Exploration." AAS 06-072. Breckenridge, CO, 4-8 Feb. 2006.

[8]   Cruz, J.R., and Lingard, J.S., "Aerodynamic Decelerators for Planetary Exploraiton: Past, Present, and Future," AIAA Guidance, Navigation, and Control Conference and Exhibit, Keystone, CO, 21-24 August 2006.

[9]   Braun, R. D., Mitcheltree, R. A., and Cheatwood, F. M., "Mars Microprobe Entry-to-Impact Analysis." Journal of Spacecraft & Rockets, Vol. 36, No. 3, May-June 1999, pp. 412-420.

[10]   Drake, B.G., "Reference Mission Version 3.0, Addendum to the Human Exploration of Mars: The Reference Mission of the NASA Mars Exploration Study Team," NASA Johnson Space Center, EX13-98-036, June 1998.

[11]   Kanacke, T.W., "Parachute Recovery Systems Design Manual," NWC TP 6575, Para Publishing, 1992.

[12]   Griffin, B., Thomas, B., Vaughan, D., Drake, B., Johnson, L., Woodcock, G., "A Comparison of Transportation Systems for Human Mission to Mars," AIAA-2004-3834, 40th AIAA/ASME/SAE/ASEE Joint Propulsion Conference and Exhibit, Fort Lauderdale, FL, 11-14 July 2004.

[13]   Cruz, J.R., "Opening Loads Analyses for Various Disk-Gap-Band Parachutes," 17th AIAA Aerodynamic Decelerator Systems Technology Conference and Seminar, 19-22 May 2003, Monterey, California.

[14]   Humble, R.W. Henry, G.N., Larson, W.J., "Space Propulsion Analysis and Design," McGraw-Hill Companies, 1995.

[15]   Larson, W.J. and Pranke,L.K., "Human Spaceflight Analysis and Design," McGraw-Hill Companies, 1999.

[16]   Hofstetter, W., de Weck, O., and Crawley, E., "Modular Building Blocks for Manned Spacecraft: A Case Study for Moon and Mars Landing Systesm," INCOSE, 2005.

[17]   "NASA's Exploration Systems Architecture Study," NASA-TM-2005-214062, November 2005.